JACS
JOURNAL OF THE AMERICAN CHEMICAL SOCIETY
Article
pubs.acs.org/JACS

Exploiting Differential Surface Display of Chondroitin Sulfate Variants for Directing Neuronal Outgrowth

Vimal P. Swarup,[†] Tony W. Hsiao,[†] Jianxing Zhang,[‡] Glenn D. Prestwich,[‡] Balagurunathan Kuberan,*[,‡,§] and Vladimir Hlady*[,†]

[†]Department of Bioengineering, [‡]Department of Medicinal Chemistry, and [§]Interdepartmental Program in Neuroscience, University of Utah, Salt Lake City, Utah 84112, United States

Supporting Information

ABSTRACT: Chondroitin sulfate (CS) proteoglycans (CSPGs) are known to be primary inhibitors of neuronal regeneration at scar sites. However, a variety of CSPGs are also involved in neuronal growth and guidance during other physiological stages. Sulfation patterns of CS chains influence their interactions with various growth factors in the central nervous system (CNS), thus influencing neuronal growth, inhibition, and pathfinding. This report demonstrates the use of differentially sulfated CS chains for neuronal navigation. Surface-immobilized patterns of CS glycosaminoglycan chains were used to determine neuronal preference toward specific sulfations of five CS variants: CS-A, CS-B (dermatan sulfate), CS-C, CS-D, and CS-E. Neurons preferred CS-A, CS-B, and CS-E and avoided CS-C containing lanes. In addition, significant alignment of neurites was observed using underlying lanes containing CS-A, CS-B, and CS-E chains. To utilize differential preference of neurons toward the CS variants, a binary combinations of CS chains were created by backfilling a neuro-preferred CS variant between the microcontact printed lanes of CS-C stripes, which are avoided by neurons. The neuronal outgrowth results demonstrate for the first time that a combination of sulfation variants of CS chains without any protein component of CSPG is sufficient for directing neuronal outgrowth. Biomaterials with surface immobilized GAG chains could find numerous applications as bridging devices for tackling CNS injuries where directional growth of neurons is critical for recovery.

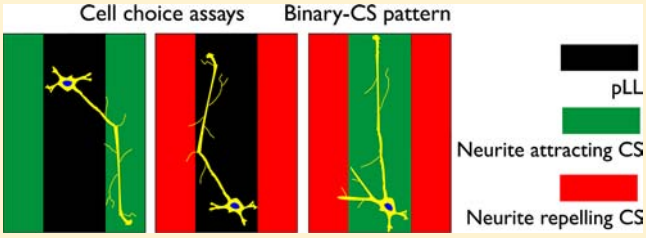

INTRODUCTION

Chondroitin sulfates are linear, sulfated glycosaminoglycans (GAG) attached to core proteins of CS proteoglycans. Numerous studies have shown that CS is the primary inhibiting GAG type found at central nervous system (CNS) injury sites.[1−3] CSPGs are upregulated in barrier tissues and glial scar regions,[4,5] which have been shown to coincide with outgrowth terminations of dorsal root ganglion (DRG) neurons.[6] Even though CSPGs are known inhibitors of axonal growth, some sulfation variants of CS have been found in developing, growth-permissive regions of the CNS,[7,8] and CS chains can also stimulate the growth of neurons.[9−11] The sulfation motifs of different CS chains are not uniform, and even subtle differences in their composition can affect the function of corresponding CSPG in the CNS.[12] Some literature reports either dispute the functional significance of the sulfation motifs present in CS chains or provide contradictory evidence for the role of sulfation variants in neuronal regeneration, plasticity, and recovery.[12−17] Recently, Brown et al. addressed this by chemically synthesizing homogeneous glycopolymers of CS-A, CS-C, and CS-E disaccharide motifs and examining their role in axonal regeneration.[18] By culturing DRG neurons on substrates containing such covalently bound glycopolymers, they showed that CS-E glycopolymers inhibited neurite outgrowth, while CS-A and CS-C had minimal activity. Sugiura et al. utilized chemo-enzymatic techniques to synthesize a library of CS molecules with well-defined sulfate compositions, and showed the sulfate dependent interactions of CS with antibodies and growth factors.[19] Table 1 summarizes the varying responses of neurons to CS sulfation patterns. Sulfation pattern seems to control molecular interactions of the CS chains, which could in part be responsible for the diverse CS roles in the CNS. Although it is clear that each CS variant influences neuronal growth differently, a systematic comparison of all CS variants, in a single study, had never been conducted. Here, we compare all five sulfation variants of CS to understand their role in neuronal pathfinding. Further, we describe a novel approach for creating neuron-guiding substrates by utilizing the differential influences of CS variants on neuronal elongation.

Since most naturally derived polysaccharides are heterogeneous, determining the structure−activity relationship among specific CS motifs becomes confounding. In this study all five major CS sulfation variants found in mammalian brain: CS-A, CS-B (dermatan sulfate), CS-C, CS-D, and CS-E, were assessed for their sulfation content and affect on neuronal pathfinding. Cell choice assays, comprising of 15 μm wide immobilized CS stripes patterned by microcontact printing (μCP) on poly-L-

Received: June 6, 2013
Published: August 15, 2013

   dx.doi.org/10.1021/ja4056728 | J. Am. Chem. Soc. 2013, 135, 13488−13494

Table 1. Influence of CS Variants on Neuronal Growth and Guidance

CS variant	sulfation or disulfation	observed effect on neurons	ref
CS-A	4S	presented negative guidance and growth cues to cerebellar granule neurons	12
CSA/CSB/CSE	4S	stimulated neurosphere formation in EGF dependent mouse embryonic neuronal stem cells	22
CS-B/CS-D/CS-E	4S	CS-B and CS-E significantly promoted FGF-2 mediated cell proliferation. CS-D led to a slight increase in proliferation	1
CS-E/CS-B	4S	interacts with pleiotrophin; promoted neurite outgrowth in hippocampal neurons by interacting with pleiotrophin	4, 23
CS-C	6S	expressed in barrier tissues to axons in avian embryo; upregulated after CNS injury; up regulation was associated to axonal regeneration in nigrostriatal axons of mice; resulted in schwann cell motility	5, 14−16
CS-D/CS-E	2S,4S or 4S,6S	promoted growth in embryonic rat hippocampal neurons	24
CS-E	4S,6S	stimulated outgrowth in neurons by binding to several CNS growth factors; assembled neurtophin-Trk complex; inhibited rat cortical cell binding by interacting with midkine, inhibited hippocampal neurons	11, 18, 25−30

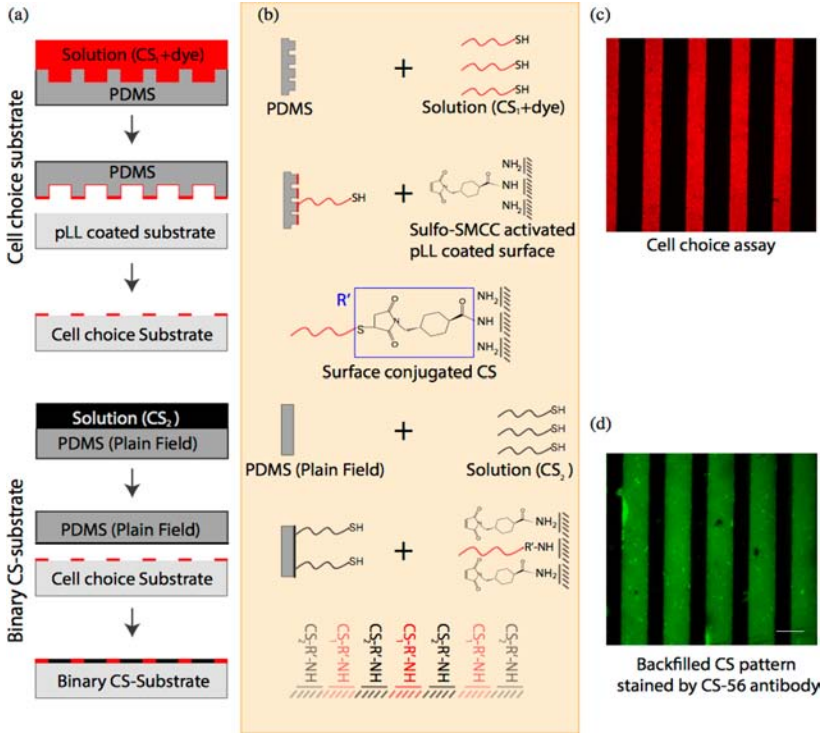

Figure 1. CS immobilization process and assay substrates. (a) Scheme for creating cell choice and binary CS-substrates. The cell choice assay comprised of 15 μm wide lanes of CS μC printed on pLL coated glass surface. In binary-CS substrates, the first CS was printed on preactivated pLL and then backfilled with the second CS. (b) Surface chemistry involved in conjugating CS to preactivated pLL coated glass surface. Each reaction step shown corresponds to the μC printing step shown in part a. Overall, μCP of thiolated CS chains onto sSMCC-activated pLL resulted in a covalent attachment of CS chains. (c) Patterned substrate for cell choice assay with CS stripe containing colocalized AlexaFluor 594 (red) flanked by pLL lanes (black). (d) The image confirms the presence and spatial localization of second, backfilled CS chains in the binary CS-substrate (Note: here CS-C was used for backfilling of CS-A lanes and was labeled by CS-56 antibody to confirm the presence and spatial localization of second CS chains) (scale bar = 25 μm).

lysine (pLL) coated substrates, were used here to determine the role of CS sulfation variants on elongating neurons. Similar cell choice assays have been previously used in other neuronal studies; however, these assays were either based on protein or proteoglycan surface patterns.[20,21] Therefore, the exclusive functionality of GAG chains on neuronal pathfinding remains to be characterized. To enhance neuronal guidance observed in the cell choice assay, CS variants having contrasting influence on neurons (permissive vs nonpermissive) were patterned sequentially to create a binary combination of CS stripes (so-called "binary-CS substrates") without any exposed pLL. To the best of our knowledge, these are the first GAG-based substrates that investigate and exploit CS variants to direct neuronal pathfinding.

MATERIALS AND METHODS

Materials. CS-A (cat. no. C9819) and CS-B (cat. no. C3788) were from Sigma Aldrich. CS-C (cat. no. C21355) was obtained from Pfaltz and Bauer, Inc. CS-D (cat. no. 400676) and CS-E (cat. no. 400678) were from Seikagaku Corp. (Tokyo, Japan). Sulfosuccinimidyl 4-[*N*-maleimidomethyl]cyclohexane-1-carboxylate (cat. no. 22122) (sSMCC) was from Thermo Scientific. AlexaFluor 594 hydrazide (cat. no. A10438) was from Invitrogen. CS-56 antibody was from Sigma-Aldrich (cat. no. C8035). Embryonic day-18 primary rat hippocampal cells (cat. no. PC35101) were purchased from Neuromics Inc.

Compositional Analysis of CS Variants. Fifty micrograms of CS chains were digested with chondroitinase ABC (5 mU, Seikagaku Corp.) in 100 μL of buffer (70 mM CH_3COONa; 0.2% BSA, pH 6.0). The mixture was incubated for 12 h at 37 °C. The resulting disaccharides were then analyzed using a strong anion-exchange

dx.doi.org/10.1021/ja4056728 | J. Am. Chem. Soc. 2013, 135, 13488−13494

(SAX)-HPLC column coupled to a UV detector. The disaccharides were eluted at a flow rate of 1 mL/min and resolved with a linear gradient of 0 to 100% solvent B (800 mM NaH_2PO_4) in solvent A (100 mM NaH_2PO_4) over 40 min. CS disaccharide standards (Seikagaku Corp. cat. no. 400571) were used for characterizing the disaccharide composition of CS variants. Results of the compositional analyses of five CS variants are presented in Supporting Information (Figure S1, SI).

Thiolation of CS Variants for Surface Immobilization. To conjugate CS chains on the pLL coated glass coverslip surfaces, thiolation of CS was performed by chemically modifying CS chains with 3,3′-dithiobis(propionic hydrazide) (DTP) using modifications of the literature protocol.[31] The degree of thiolation in CS chains was controlled by varying the amount of the CS during the reaction and was analyzed by nuclear magnetic resonance (NMR). Molecular weight assessment was done using gel permeation chromatography (Figure S2, SI).

Microcontact Surface Printing of Thiolated CS Variants (μCP). Soft lithography PDMS stamps were made using standard lithography techniques (Figure 1a).[32] The pLL coating of coverslips was conducted by placing sterile coverslips with 1.5 mL of pLL solution (0.05 mg/mL solution in water) for 1 h at room temperature (r.t.). Next, the pLL solution was removed, and coverslips were rinsed with water. sSMCC activation of pLL-coated coverslips was done by placing 700 μL of solution of sSMCC (0.8 mg/mL in activation buffer: 0.1 M $NaHPO_4$, 0.15 M NaCl, pH 7.2) on coverslips and incubating at r.t. for 1 h. Thiolated CS solution (15 μL of 1 mg/mL), premixed with 10 μL of 1 mg/mL AlexaFluor 594 in DMSO to colocalize the dye with the CS, was evenly spread over PDMS stamp and left for 20 min at r.t. Afterward, stamps were rinsed with water, dried, and placed over sSMCC-activated surfaces for 2 min. The coverslips were left for 8 h at r.t. for complete reaction (Figure 1b–c).

Binary-CS substrate was created by backfilling freshly printed CS stripes pattern with a second CS variant, which reacted with sSMCC-activated surface areas present in the unstamped lanes in between the original CS stripes. Coverslips were left for another 8 h at r.t. to complete the reaction.

Cell Culture. The dissociated hippocampal cells were pelleted by centrifugation and suspended in NbActiv1 media (cat. no. NBActiv1-100, BrainBits). Two milliliters of 8×10^4 cells/mL solution was placed into each well of a six-well plate containing the CS patterned coverslips. Neuronal culture was maintained at 37 °C and 5% CO_2. After reaching the desired time point, cells were fixed and stained with DAPI, chicken antirat TAU/MAPT primary antibody (Neuromics, CH22113) and labeled with goat antirat IgG secondary antibody conjugated to AlexaFluor 488 (Molecular Probes, A11039).

Imaging and Analysis. Fluorescent images were collected with an Olympus FV1000 IX81 microscope using a Planapo oil immersion 60× objective, NA1.42. The confocal aperture was set to one airy unit, and these settings were maintained between comparable samples. DAPI, AlexaFlour 488, and AlexaFluor 594 were excited using a 405 nm, 488 nm, and 543 nm lasers lines, respectively. Acquisition software used was FVASW V 2.1. Forty to fifty neurons (not contacting other neurons or neurites) were imaged for statistical analysis. Primary neurites were defined as the processes extending from neuronal cell body. Confocal images were level adjusted using the Photoshop software under identical settings and processed in NIH ImageJ v 1.43U using the "despeckle" noise filter. Images were analyzed using NIH ImageJ for quantitative analysis of neuronal morphology using segmented line and angle tools. Each experiment was performed in triplicate. Statistical analysis was by Anova (Kaleidagraph, Synergy Software).

Antibody-Based Confirmation of CS Containing Patterns. Immobilized CS patterns were blocked with 4% goat serum and 0.1% sodium azide in PBS for 1 h and incubated with primary antibody CS-56 at 1:500 dilution for CS-C and 1:50 dilution for CS-A. The surfaces were rinsed three times with PBS, and appropriate dye-conjugated secondary antibody (Molecular Probes) was applied at dilution of 1:500 and incubated for 1 h. The secondary antibody was rinsed three times with PBS, and the patterns were imaged using Nikon Diaphot 200 microscope with 40× objective, NA1.40 (Figure S3, SI).

To confirm the presence of CS in backfilled regions of binary-CS substrates, CS-C chains were backfilled between CS-A stripes pattern. CS-56 antibody applied at dilution of 1:500, followed by appropriate dye-conjugated secondary antibody, stained 25 μm wide lanes backfilled with CS-C only while leaving the CS-A lanes unlabeled (Figure 1d).

RESULTS

Sulfation Pattern Influences Neuronal Pathfinding. In preliminary experiments, neurons grown over plain fields of CS chains showed different growth behavior with varying CS sulfation (Figure S4, SI). Hence, a cell choice assay was used to determine the ability of the CS variants to guide neurons (Figure 1c). Representative images of neurons at 48 h time point are shown in Figure 2. The neurites strongly preferred to

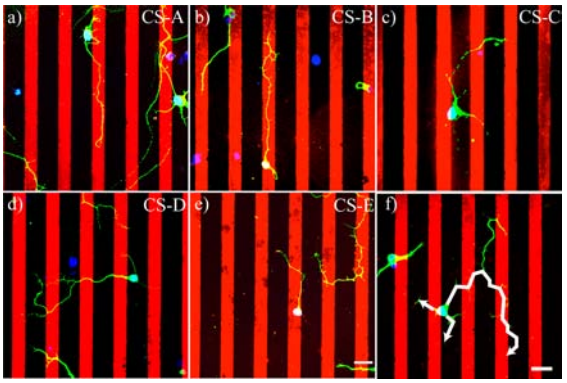

Figure 2. Neurons preferred CS-A, CS-B, and CS-E, avoided CS-C, and were neutral to CS-D. (a–e) Representative images of neurons and underlying CS patterns. Neurites preferred growing over CS-A, CS-B, and CS-E stripes, while those elongating over the CS-C patterned surfaces preferred pLL lanes. (f) Approach used for measuring neurite length of neurons. All primary neurites were mapped and measured using segment line tool of ImageJ software. When primary neurites branched, only the longest neurite was used for quantification. (Scale bar = 25 μm, green: antirat TAU/MAPT, blue: DAPI, red: AlexaFluor 594 colocalized with CS's).

grow on CS-A and CS-B, while they had a mild preference for CS-E (Figure 2a,b,e). In contrast, CS-C had an opposite effect on neurites: they preferred to grow on the pLL lanes and avoided CS-C stripes (Figure 2c). Neurons did not show any directional response to CS-D pattern (Figure 2d).

A statistical comparison of the neurite lengths found on the CS stripes at the 48 h time point is shown in Figure 3a; the average neurite length was shortest for CS-C and longest for CS-B stripes. Neurite lengths on pLL regions of five CS cell choice substrates were statistically identical (data not shown). When the fractions of neurites localized on the CS regions were plotted against the 6S/4S sulfation ratio of each CS variant, the results revealed that the neuronal preference for a given CS variant (as indicated by higher fraction of neurites on CS stripe) decreased with increasing 6S/4S ratio (Figure 3b).

To validate the sulfation-dependent contrast observed in neuronal preference, we conducted cell choice assays on mixtures of CS-B and CS-C in varying proportions: 90% CS-B and 10% CS-C (90B:10C); 50% CS-B and 50% CS-C (50B:50C); 10% CS-B and 90% CS-C (10B:90C), Figure S5, SI. As evident from Figure S5, neurons strongly preferred a low 6S/4S mixture (90B:10C) and avoided a high 6S/4S sample

dx.doi.org/10.1021/ja4056728 | J. Am. Chem. Soc. 2013, 135, 13488–13494

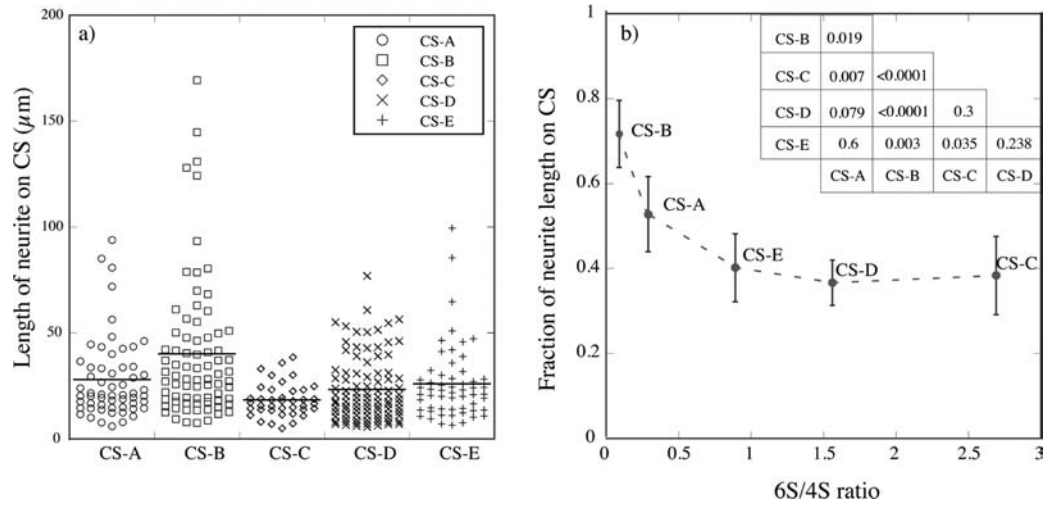

Figure 3. Neurons avoid of CS's with a high 6S/4S ratio. (a) The length of neurite segments localized on the CS stripes at 48 h. The black lines represent the average neurite length. The insert table in b shows the corresponding *p*-values. (b) The fraction of neurite length on CS lanes vs the 6S/4S sulfation ratio of corresponding CS chains at 48 h. The 6S/4S sulfation ratios took both mono and disulfated 6S or 4S residues into account. The increase in 6S/4S ratio resulted in the avoidance of the CS stripes by neurons. The error bar corresponds to SEM with 95% confidence.

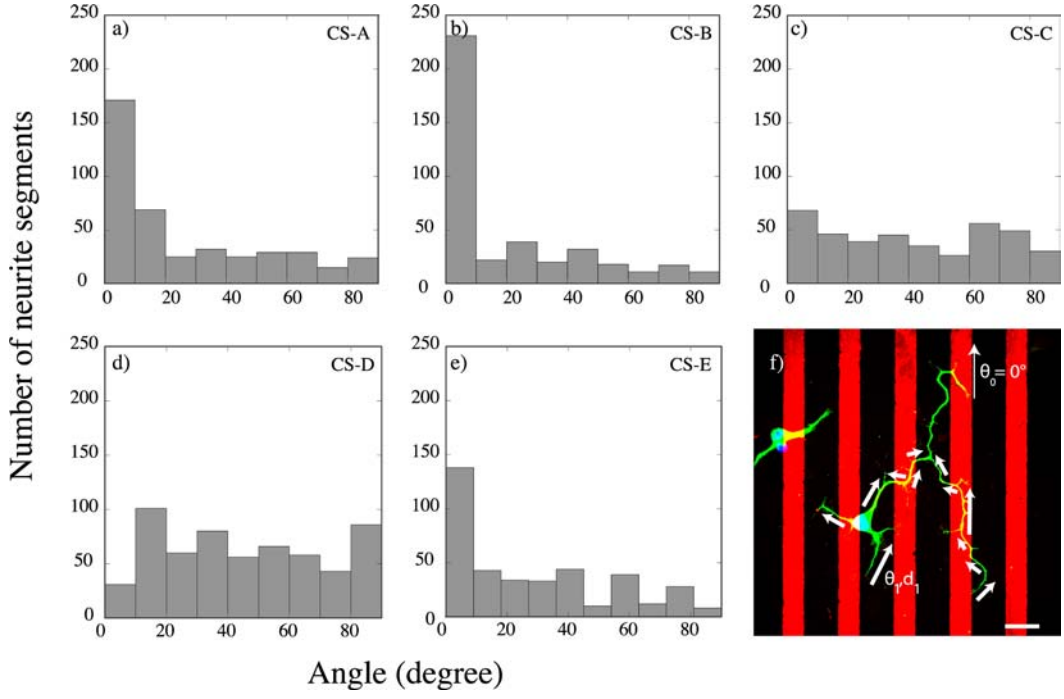

Figure 4. Neurons aligned parallel to CS-A, CS-B, and CS-E stripes. (a–e) Each histogram presents the angle distribution made by 10 μm long neurite segments and the CS stripes at 48 h. Neurites aligned with the underlying CS-A, CS-B, and CS-E lanes and not with either CS-C or CS-D lanes. (f) Approach used for analyzing neuronal alignment by creating histogram. Primary neurites were divided in straight segments. The length and acute angle formed by segments and CS stripes were measured using angle tool of ImageJ. The frequency of a given angle was assigned by calculating the number of 10 μm units present in the corresponding neurite segment. Scale bar = 25 μm, green: antirat TAU/MAPT, blue: DAPI, red: AlexaFluor 594 colocalized with CSs.

(10B:90C). Alignment of the neurites with the CS stripes was quantified at the 48 h time point by mapping the angle made between 10 μm-long neurite segments and the underlying CS stripes, creating angle histograms shown in Figure 4 (24 h data are shown in Figure S6, SI). The skew of the histograms toward low angles (indicating alignment) was observed for CS-A, CS-B, and CS-E stripes. The CS-D and CS-C stripes did not cause any alignment of neurites. Neurons on CS-E printed substrates showed a mild preference for CS; hence they elongate along the CS-E/pLL boundary, aligning with the underlying stripes (Figures 2e, 3a, and 4e).

Binary-CS Substrates Enhance Neuronal Guidance. The differential response of neuronal growth to various CS chains was utilized to create binary-CS substrates containing alternate lanes of neurite repelling (CS-C) and aligning (CS-A, CS-B, and CS-E) GAG chains, with no pLL exposed. The binary substrates were created by backfilling CS-C cell choice substrates with CS-A, CS-B, or CS-E chains, respectively. The presence of second CS variant in backfilled regions in between

dx.doi.org/10.1021/ja4056728 | J. Am. Chem. Soc. 2013, 135, 13488–13494

the originally printed first CS variant was confirmed by antibody staining (Figure 1d). Thus, the binary-CS substrates contained alternating 15 μm wide lanes of CS-C separated by 25 μm wide lanes of CS-A, CS-B, or CS-E chains. Figure 5a–c represents typical neuronal growth response to the binary-CS substrates. Neurites aligned parallel to permissive CS stripes (CS-A, CS-B, or CS-E) and avoided crossing CS-C lanes.

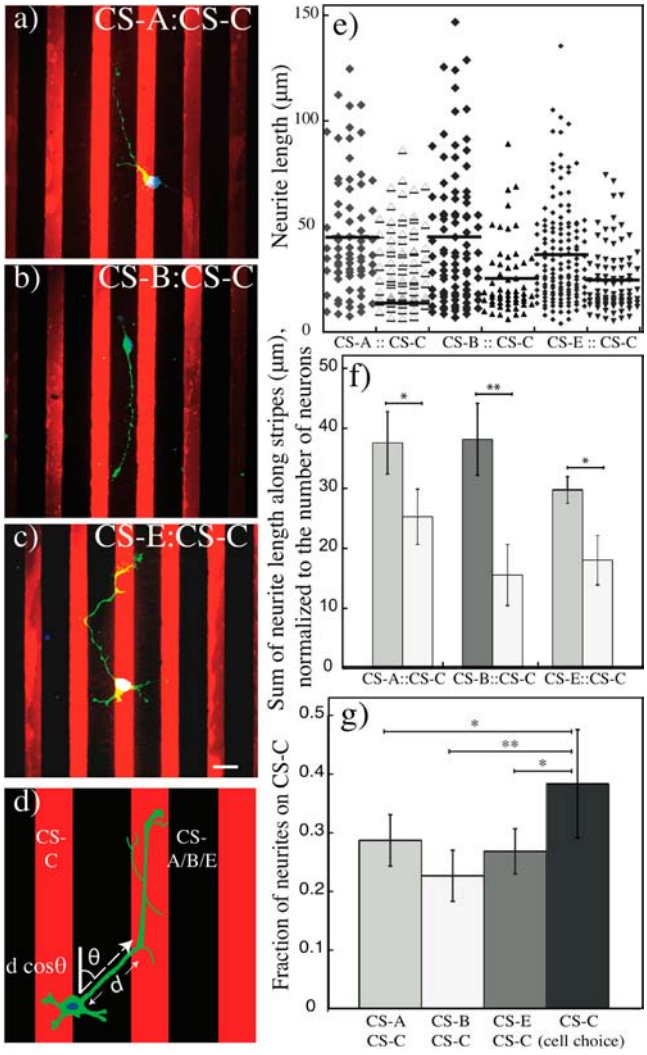

Figure 5. Neuronal guiding substrate created by a binary-CS pattern. A binary-CS pattern was created to copresent two CS variants having contrasting influence on neuronal pathfinding. The binary-CS patterned substrates were generated by microcontact printing of CS-C lanes on preactivated PLL (red) and then backfilling it with CS-A, CS-B, or CS-E chains (black), as described in Figure 1. (a–c) Representative images of neuronal growth pattern after 48 h on binary patterns consisting of CS-A:CS-C, CS-B:CS-C, and CS-E:CS-C chain combinations.(d) Approach used for analyzing neurite length along lanes. (e) Length of the neurites on each of the three binary-CS patterns. (f) Sum of neurite length resolved along stripe, normalized to the number of neurons. The gray bars represent neurite length on CS-A, CS-B, and CS-E lanes, while the white bars represent neurite length on CS-C lanes in each combination. Error bars represent standard deviation of three independent experiments. (g) Comparison of fractional length of neurites on CS-C in binary-CS substrates and in CS-C vs pLL cell choice assay. Error bar corresponds to SEM with 95% confidence. Scale bar = 25 μm, green: antirat TAU/MAPT, red: AlexaFluor 594 colocalized with CS-C, *p < 0.01; **p < 0.001.

Figure 5e shows the length of neurites on the CS stripes. To compensate for different stripe widths (25 μm for CS-A/B/E vs 15 μm for CS-C), the neurite lengths parallel to the stripes were obtained by taking their cosine components and compared as shown in Figure 5f. The gray bars represent neurite length on CS-A, CS-B, and CS-E, and the white bar shows the neurite length on CS-C stripes in each combination. The results showed that neurites preferred to grow on permissive regions (CS-A, CS-B, or CS-E) while avoiding barrier lanes (CS-C). The CS-B:CS-C binary pattern showed the best alignment profile among the three combinations. Figure 5g shows the aligning efficiency of binary-CS patterns by comparing fractional length of neurites localized on CS-C stripes in binary-CS patterns with the fractional lengths found in CS-C cell choice assay (i.e., on CS-C + pLL lanes pattern, Figure 2c). Neurite localization on that CS-C cell choice assay was ~38%, which dropped to 28% in CS-A:CS-C, 23% in CS-B:CS-C, and 27% in CS-E:CS-C binary patterns, respectively. Thus, it is evident that the two copresented CS variants acted synergistically to guide neurons with efficiency greater than the single CS patterns in the cell choice assays.

■ DISCUSSION

By playing crucial roles in CNS signaling, GAGs have the potential to control neuronal growth and guidance and, hence, can be used to develop novel biomaterials. Although several studies have attempted to decipher the role of various sulfation motifs of CS chains,[11,14,18,25,33,34] this is the first report on the individual contribution of sulfation patterns on neuronal pathfinding. In the present study, CS chains were immobilized by reacting their thiol moiety to preactivated pLL surfaces using μCP. To determine the influence of CS sulfate motifs on neuronal pathfinding, five CS variants that have dominant sulfate groups at different positions (2S; 4S; 6S; 2S,4S; 2S,6S and 4S,6S) were used. Each CS variant showed the predominance of one sulfate motif (except CS-D); however, the presence of lower amounts of other sulfate motifs was also observed (SI, Figure S1). These sulfate motifs may indicate how the role of the CSPGs changes with a particular stimulus (i.e., development or injury) because CS variants have been known to influence the CNS in multiple ways, including: neuronal growth, migration, differentiation, pathfinding, and maturation.[3,35,36] Each CS variant was subjected to minimal thiolation of the glucuronyl carboxylic acid moiety such that approximately 1 or 2 out of every 100 disaccharide residues was modified. Such minimal modification was necessary to preserve the recognition sites on the CS chains for CS-recognizing proteins present on the neuronal cell surface.

Neurons analyzed for cell growth on plain fields of CS variants differed in the extent of neurite outgrowth (SI, Figure S4). The neurites were longest for neurons grown over CS-D and shortest for the CS-C surfaces. This result conforms with the previous findings about up-regulation of CS-C after spinal cord injuries which prevents neuronal outgrowth and regeneration, while CS-A, CS-D, and CS-E have stimulatory effect on neuronal outgrowth.[14] CS-C is implicated in disrupting pleotrophin-induced neurite outgrowth by inhibiting the phosphacan-pleotrophin interaction, whereas CS-A is a poor inhibitor of this interaction.[37] A weak inhibition or, in some cases, a mild stimulation of neurite growth has been reported for CS-A on laminin, or on L1 glycoprotein coated surfaces, respectively.[38] CS-D and CS-E have previously been shown to promote neurite outgrowth in rat hippocampal

dx.doi.org/10.1021/ja4056728 | J. Am. Chem. Soc. 2013, 135, 13488–13494

neurons. Furthermore, it is also known that both CS-D and CS-E bind directly to selectins, chemokines, and midkine with high affinity, indicating that these CS variants may also be involved in multiple neuro-regulatory functions such as adhesion, migration, guidance, and neurite outgrowth.[19,25,34,39]

Based on the observation that CS sulfation variants caused differing responses of neuronal outgrowth, we hypothesized their varying influences on neuronal pathfinding as well. The analysis of cell choice assays results when combined with the CS sulfation profile of each CS variant revealed that neuronal preference for CS chains decreases with the increasing ratio of 6S/4S sulfations in the CS (Figure 3b). The role of 6S/4S sulfation ratio was further confirmed by using neuronal cell choice assays with stripes made by three different CS-B + CS-C mixtures on pLL (Figure S5, SI). Miyata et al. have recently shown that developmental increase in 4S/6S sulfation ratio results in termination of critical periods of plasticity in mouse visual cortex.[40] However, to the best of our knowledge, this is the first study that shows the correlation between 6S/4S sulfation ratio and neuronal pathfinding. Brown et al. used homogeneous synthetic glycopolymers of CS-A (100% 4S), CS-C (100% 6S), and CS-E (100% 4S, 6S) motifs and examined their role in axonal regeneration of dorsal root ganglions (DRGs).[18] They observed that CS-E glycopolymers inhibited neurite outgrowth, while CS-A and CS-C had minimal activity. The same lab has previously shown that CS-E tetrasaccharide stimulated neurite outgrowth of hippocampal neurons by 49%, whereas CS-A and CS-C had no appreciable activity.[11] The opposing effect of CS-E chains on two different neuronal cell types (DRG vs hippocampal neurons) indicates that the influence of CS chains on neuronal pathfinding could be variable for different neuronal cell types, or between the CNS and the peripheral nervous system neurons.

We observed the alignment of the neurites on CS-A and CS-B stripes which were previously not found to be effective in neuronal alignment (Figure 4).[11,25] The alignment of neurons found in this study was largely determined by the dominant CS sulfation motifs. The presence of 4S motifs appears to be required for preferential growth alignment of neurons. Another important finding from the present study is the inhibitory effect of the dominant 6S sulfation motif of CS-C chains. Even though the 6S sulfation motifs were also present in CS-D, the neurons did not align but proliferated well over CS-D surfaces (Figure 2 and Figure S4, SI). It is plausible that observed cellular response to sulfation motifs is very sensitive to the amount of 6S motifs present in each GAG (for example, there is 55% of 6S in CS-C vs 37% in CS-D). Interestingly, Wang et al. showed that a small change in the sulfate content of CS-A could drastically affect its inhibitory potential.[12] This suggests that even modest changes in relative sulfate content can have profound effects upon neurons and supports our conclusion regarding the differential influence of sulfation motifs.

Considering that the composition of each CS variant is not exclusively dominated by one sulfation motif, the present study showed that a subtle difference in the composition of CS sulfation motifs could lead to significant changes in neuronal pathfinding. These differences have been shown to be central in various physiological processes including perineuronal net functioning, which have CS as one of the major constituents.[40] Changes in CS-E expression have also been associated with spinal cord injury.[14] Transient yet precise and marked changes of sulfation motifs of CS, known to take place during early development,[41,42] may also be responsible for regulating the balance between the inhibitory and permissive stimuli for elongating neurons.

Based on the results of the cell choice assay (Figure 2), we designed a novel CS-only based strategy for axonal guidance. The response of the neuronal pathfinding to the 6S/4S sulfation ratio was used to create a binary-GAG substrate that could mediate directional growth of neurons with high fidelity (Figure 5). Since CS-C was the most growth inhibitory and neurite repelling CS variant, its stripes were used as barriers for elongating axons. Neurite aligning CS-A, CS-B or CS-E lanes were created to flank these CS-C barrier stripes. By depositing alternating stripes of two CS chains, containing wider cell permissive regions interspaced with narrower barrier lanes, we demonstrated a unique approach for enhancing neuronal alignment. It must be noted that, while CS-C and CS-E stripes have similar fractional length of neurites localizing on them (Figure 3b), the two CS variants showed opposite effects toward neurite alignment in cell choice assays (Figure 4c,e). However, a binary combination of CS-C and CS-E chains facilitated preferential growth of neurites on CS-E lanes while avoiding CS-C stripes (Figure 5c, $p < 0.01$). CS-B:CS-C combination, with its biggest difference in respective 6S/4S ratios, was observed to have the most effective neuronal alignment. Thus, differential response of neurites toward CS variants allowed us to engineer effective substrates for directional growth of neurites solely based on the CS variants. The results of this study demonstrate that a combination of substrate presented CS variants can be used to guide neurons with high efficiency and be used for developing bridging devices for CNS injuries that require providing directional cues to elongating neurons.

■ CONCLUSIONS

The present study utilized differences in CS sulfation to create neuron-aligning substrates. We determined the role of CS sulfation motifs on neuronal pathfinding by using five CS variants in cell choice assay. The cell choice assay demonstrated preferential growth and alignment of neurons on CS-A, CS-B, and CS-E stripes vs pLL surfaces and an opposite response toward CS-C striped substrate. The cell alignment suggested that the dominant 4S motif of these CS chains plays a critical role in neuronal guidance. The sulfate dependent neuronal pathfinding response was exploited to create novel binary-CS patterns for guiding neurites. Cell aligning CS chains (CS-A, CS-B, or CS-E) were copresented with CS-C chains that were avoided by neurites. The alignment was most effective in substrate presenting a CS-B:CS-C combination. The directional growth of neurons over CS-B and their avoidance of the CS-C stripes demonstrated that the copresentation of CS chains is a potentially useful approach to create unique biomaterials to support neuronal pathfinding and regeneration.

■ ASSOCIATED CONTENT

Ⓢ Supporting Information

Characterization of thiolated CS, antibody staining to confirm CS surface immobilization, cell growth assay, cell choice assay at 24 h, and cell choice assay on CS-B/CS-C mixtures. This material is available free of charge via the Internet at http://pubs.acs.org.

■ AUTHOR INFORMATION

Corresponding Authors

vladimir.hlady@utah.edu

kuby@pharm.utah.edu

Notes

The authors declare no competing financial interest.

■ ACKNOWLEDGMENTS

The study was supported by NIH Grant (R01 NS57144). The authors are thankful to Dr. P. Tresco for valuable suggestions and to V. M. Tran, C. Rodesch, and C. Eichinger for providing experimental assistance required for the study.

■ REFERENCES

(1) Ida, M.; Shuo, T.; Hirano, K.; Tokita, Y.; Nakanishi, K.; Matsui, F.; Aono, S.; Fujita, H.; Fujiwara, Y.; Kaji, T. *J. Biol. Chem.* **2006**, *281*, 5982.
(2) Silver, J.; Miller, J. H. *Nat. Rev. Neurosci.* **2004**, *5*, 146.
(3) Swarup, V. P.; Mencio, C. P.; Hlady, V.; Kuberan, B. *BioMol. Concepts* **2013**, *4*, 233.
(4) Bao, X.; Muramatsu, T.; Sugahara, K. *J. Biol. Chem.* **2005**, *280*, 35318.
(5) Oakley, R. A.; Tosney, K. W. *Dev. Biol.* **1991**, *147*, 187.
(6) Davies, S. J. A.; Fitch, M. T.; Memberg, S. P.; Hall, A. K.; Raisman, G.; Silver, J. *Nature* **1997**, *390*, 680.
(7) Bicknese, A. R.; Sheppard, A. M.; O'leary, D. D.; Pearlman, A. L. *J. Neurosci.* **1994**, *14*, 3500.
(8) Faissner, A.; Clement, A.; Lochter, A.; Streit, A.; Mandl, C.; Schachner, M. *J. Cell Biol.* **1994**, *126*, 783.
(9) Nadanaka, S.; Clement, A.; Masayama, K.; Faissner, A.; Sugahara, K. *J. Biol. Chem.* **1998**, *273*, 3296.
(10) Maeda, N.; Ishii, M.; Nishimura, K.; Kamimura, K. *Neurochem. Res.* **2010**, *36*, 1228.
(11) Tully, S. E.; Mabon, R.; Gama, C. I.; Tsai, S. M.; Liu, X.; Hsieh-Wilson, L. C. *J. Am. Chem. Soc.* **2004**, *126*, 7736.
(12) Wang, H.; Katagiri, Y.; McCann, T. E.; Unsworth, E.; Goldsmith, P.; Yu, Z. X.; Tan, F.; Santiago, L.; Mills, E. M.; Wang, Y.; Symes, A. J.; Geller, H. M. *J. Cell Sci.* **2008**, *121*, 3083.
(13) Karumbaiah, L.; Anand, S.; Thazhath, R.; Zhong, Y.; Mckeon, R. J.; Bellamkonda, R. V. *Glia* **2011**, *59*, 981.
(14) Properzi, F.; Carulli, D.; Asher, R. A.; Muir, E.; Camargo, L. M.; Van Kuppevelt, T. H.; Ten Dam, G. B.; Furukawa, Y.; Mikami, T.; Sugahara, K.; Toida, T.; Geller, H. M.; Fawcett, J. W. *Eur. J. Neurosci.* **2005**, *21*, 378.
(15) Lin, R.; Rosahl, T. W.; Whiting, P. J.; Fawcett, J. W.; Kwok, J. C. F. *PLoS One* **2011**, *6*, e21499.
(16) Liu, J.; Chau, C. H.; Liu, H.; Jang, B. R.; Li, X.; Chan, Y. S.; Shum, D. K. Y. *J. Cell Sci.* **2006**, *119*, 933.
(17) Shimbo, M.; Ando, S.; Sugiura, N.; Kimata, K.; Ichijo, H. *Brain Res.* **2012**, *1491*, 34.
(18) Brown, J. M.; Xia, J.; Zhuang, B. Q.; Cho, K. S.; Rogers, C. J.; Gama, C. I.; Rawat, M.; Tully, S. E.; Uetani, N.; Mason, D. E.; Tremblay, M. L.; Peters, E. C.; Habuchi, O.; Chen, D. F.; Hsieh-Wilson, L. C. *Proc. Natl. Acad. Sci.* **2012**, *109*, 4768.
(19) Sugiura, N.; Shioiri, T.; Chiba, M.; Sato, T.; Narimatsu, H.; Kimata, K.; Watanabe, H. *J. Biol. Chem.* **2012**, *287*, 43390.
(20) Frotscher, M.; Haas, C. A.; Förster, E. *Cerebral Cortex* **2003**, *13*, 634.
(21) Hodgkinson, G. N.; Tresco, P. A.; Hlady, V. *Biomaterials* **2012**, *33*, 4288.
(22) Tham, M.; Ramasamy, S.; Gan, H. T.; Ramachandran, A.; Poonepalli, A.; Yu, Y. H.; Ahmed, S. *PLoS One* **2010**, *5*, e15341.
(23) Bao, X.; Mikami, T.; Yamada, S.; Faissner, A.; Muramatsu, T.; Sugahara, K. *J. Biol. Chem.* **2005**, *280*, 9180.
(24) Sugahara, K.; Yamada, S. *Trends Glycosci. Glycotechnol.* **2000**, *12*, 321.
(25) Gama, C. I.; Tully, S. E.; Sotogaku, N.; Clark, P. M.; Rawat, M.; Vaidehi, N.; Goddard, W. A.; Nishi, A.; Hsieh-Wilson, L. C. *Nat. Chem. Biol.* **2006**, *2*, 467.
(26) Tully, S.; Rawat, M.; Hsieh-Wilson, L. *J. Am. Chem. Soc.* **2006**, *128*, 7740.
(27) Rogers, C. J.; Clark, P. M.; Tully, S. E.; Abrol, R.; Garcia, K. C.; Goddard, W. A.; Hsieh-Wilson, L. C. *Proc. Natl. Acad. Sci. U.S.A.* **2011**, *108*, 9747.
(28) Deepa, S.; Umehara, Y.; Higashiyama, S.; Itoh, N.; Sugahara, K. *J. Biol. Chem.* **2002**, *277*, 43707.
(29) Ciani, L.; Salinas, P. C. *Nat. Rev. Neurosci.* **2005**, *6*, 351.
(30) Gilbert, R. J.; McKeon, R. J.; Darr, A.; Calabro, A.; Hascall, V. C.; Bellamkonda, R. V. *Mol. Cell. Neurosci.* **2005**, *29*, 545.
(31) Liu, Y.; Cai, S.; Shu, X. Z.; Shelby, J.; Prestwich, G. D. *Wound Repair Regen.* **2007**, *15*, 245.
(32) Singhvi, R.; Kumar, A.; Lopez, G. P.; Stephanopoulos, G. N.; Wang, D.; Whitesides, G. M.; Ingber, D. E. *Science* **1994**, *264*, 696.
(33) Ishii, M.; Maeda, N. *J. Biol. Chem.* **2008**, *283*, 32610.
(34) Kawashima, H.; Atarashi, K.; Hirose, M.; Hirose, J.; Yamada, S.; Sugahara, K.; Miyasaka, M. *J. Biol. Chem.* **2002**, *277*, 12921.
(35) Brittis, P. A.; Canning, D. R.; Silver, J. *Science* **1992**, *255*, 733.
(36) Nishimura, K.; Ishii, M.; Kuraoka, M.; Kamimura, K.; Maeda, N. *Neuroscience* **2010**, *169*, 1535.
(37) Maeda, N.; Nishiwaki, T.; Shintani, T.; Hamanaka, H.; Noda, M. *J. Biol. Chem.* **1996**, *271*, 21446.
(38) Dou, C. L.; Levine, J. M. *J. Neurosci.* **1995**, *15*, 8053.
(39) Ueoka, C.; Kaneda, N.; Okazaki, I.; Nadanaka, S.; Muramatsu, T.; Sugahara, K. *J. Biol. Chem.* **2000**, *275*, 37407.
(40) Miyata, S.; Komatsu, Y.; Yoshimura, Y.; Taya, C.; Kitagawa, H. *Nat. Neurosci.* **2012**, *15*, 414.
(41) Mark, M. P.; Baker, J. R.; Kimata, K.; Ruch, J. V. *Int. J. Develop. Biol.* **1990**, *34*, 191.
(42) Kitagawa, H.; Tsutsumi, K.; Tone, Y.; Sugahara, K. *J. Biol. Chem.* **1997**, *272*, 31377.